The FASEB Journal article fj.14-266379. Published online April 17, 2015.

Mitotic quiescence, but not unique "stemness," marks the phenotype of bone metastasis-initiating cells in prostate cancer

Ning Wang,* Freyja Docherty,* Hannah K. Brown,* Kim Reeves,† Anne Fowles,* Michelle Lawson,‡ Penelope D. Ottewell,‡ Ingunn Holen,‡ Peter I. Croucher,§ and Colby L. Eaton*,[1]

*Department of Human Metabolism, Medical School, University of Sheffield, Sheffield, United Kingdom; †Breakthrough Breast Cancer Research Unit, Paterson Institute for Cancer Research, Manchester, United Kingdom; ‡Department of Oncology, Medical School, University of Sheffield, Sheffield, United Kingdom; and §Bone Biology Division, Garvan Institute of Medical Research, Sydney, Australia

ABSTRACT **This study aimed to identify subpopulations of prostate cancer cells that are responsible for the initiation of bone metastases. Using rapidly dividing human prostate cancer cell lines, we identified mitotically quiescent subpopulations (<1%), which we compared with the rapidly dividing populations for patterns of gene expression and for their ability to migrate to the skeletons of athymic mice. The study used 2-photon microscopy to map the presence/distribution of fluorescently labeled, quiescent cells and luciferase expression to determine the presence of growing bone metastases. We showed that the mitotically quiescent cells were very significantly more tumorigenic in forming bone metastases than fast-growing cells (55 *vs.* 15%) and had a unique gene expression profile. The quiescent cells were not uniquely stem cell like, with no expression of CD133 but had the same level expression of other putative prostate stem cell markers (CD44 and integrins α2/β1), when compared to the rapidly proliferating population. In addition, mitotic quiescence was associated with very high levels of C-X-C chemokine receptor type 4 (CXCR4) production. Inhibition of CXCR4 activity altered the homing of quiescent tumor cells to bone. Our studies suggest that mitotic dormancy is a unique phenotype that facilitates tumor cell colonization of the skeleton in prostate cancer.—Wang, N., Docherty, F., Brown, H. K., Reeves, K., Fowles, A., Lawson, M., Ottewell, P. D., Holen, I., Croucher, P. I., Eaton, C. L. Mitotic quiescence, but not unique "stemness," marks the phenotype of bone metastasis-initiating cells in prostate cancer. *FASEB J.* 29, 000–000 (2015). www.fasebj.org**

Key Words: cell quiescence · CXCR4 · metastatic niche

ALTHOUGH PROSTATECTOMY IS A SUCCESSFUL treatment for prostate cancer that appears to be organ confined, in a significant number of patients, the disease progresses, primarily by metastasis to the skeleton. In some cases, this occurs many years after removal of the primary cancer, so it is clear that trafficking of tumor cells in/out of the bone microenvironment occurs at an early stage in the disease in some patients. It is also likely that this continues throughout the disease and is a major driver of disease progression.

Recent studies have suggested that prostate cancers contain stem cell-like populations (1–9), and these may contribute to tumor heterogeneity and their adaptability. Others have suggested that disseminating prostate cancer cells locate to "niches" within the bone marrow, normally occupied by hematopoietic stem cells (HSCs) (10). However, the phenotype of the metastasis-initiating population remains elusive, although it is believed that metastasizing cells will be mitotically quiescent. In this state, they could survive in specific metastatic niches, and their lack of proliferation would allow them to remain undetected for extended periods of time and confer resistance to antiproliferative agents.

We have studied several human prostate cancer cell lines *in vitro* to determine if they contain subpopulations that are mitotically quiescent with metastasis-initiating potential. The cell lines were stained with vital lipophilic fluorescent dyes and followed in culture for several weeks. These dyes are very bright and, importantly, are lost as cells divide, allowing nondividing/slowly dividing cells, referred to here as quiescent, to be identified and distinguished from proliferating cells (11). Using this method, we have isolated and characterized a low-frequency, quiescent population from all cell lines. These cells or equivalent numbers of

Abbreviations: CT, cycle threshold; CXCR4, C-X-C chemokine receptor type 4; ECM, extracellular matrix; EMT, epithelial-to-mesenchymal transition; FACS, fluorescence-activated cell sorting; GAPDH, glyceraldehyde 3-phosphate dehydrogenase; GFP, green fluorescent protein; HSC, hematopoietic stem cell; i.c., intracardiac (intracardially); MCAM, melanoma cell adhesion molecule; MMP, matrix metalloproteinase; PSCA, prostate stem cell antigen; qRT-PCR, quantitative RT-PCR

[1] Correspondence: Academic Unit of Bone Biology, Department of Human Metabolism, D Floor, The Medical School, Beech Hill Rd., Sheffield S10 2RX, United Kingdom. E-mail: c.l.eaton@sheffield.ac.uk

doi: 10.1096/fj.14-266379

This article includes supplemental data. Please visit *http://www.fasebj.org* to obtain this information.

rapidly dividing cells were injected into the circulation of athymic mice, and tumor growth was assessed using bioluminescent *in vivo* imaging and postmortem histology/2-photon microscopy. We assessed the relative capacities of these populations to form skeletal tumors in these animals. We have also presented a gene expression profile for quiescent cells.

MATERIALS AND METHODS

Cell lines

The PC3 prostate cancer cell line [American Type Culture Collection (ATCC), Manassas, VA, USA] was stably transfected with a firefly luciferase gene, *luc2* [pGL4.51 (luc2/CMV/Neo) vector; Promega, Madison, WI, USA], using a Gene Pulser electroporator (Bio-Rad, Hercules, CA, USA) (denoted PC3-NW1) and transfected with Amaxa pmaxGFP vector (Lonza, Basel, Switzerland) [PC3-green fluorescent protein (GFP)]. LNCaPs were purchased from ATCC, and the C4 2B4 strain was supplied by the University of Bern (Bern, Switzerland). All cell lines were maintained in DMEM (Gibco, Life Technologies, Carlsbad, CA, USA), supplemented with antibiotics and fetal bovine serum (Sigma-Aldrich, Poole, United Kingdom). All cell lines were genetically profiled by the StemElite ID System (Promega) that confirmed their identity (18 out of 18 short tandem repeats).

Mitotically quiescent cells *in vitro*

Defining the quiescent population in vitro

Prostate cancer cells were stained in suspension with 5 μM lipophilic carbocyanine dye Vybrant DiD (Life Technologies) according to the manufacturer's instructions. The proportion of cells retaining the dye with/without a 3-hour pretreatment of 5 μg/ml Mitomycin C (Sigma-Aldrich) was analyzed by FACSCalibur (BD Biosciences, Oxford, United Kingdom). Cells were imaged using a Leica DMI 4000B microscope (Leica Microsystems, Buffalo Grove, IL, USA). The effect of lipophilic dyes on cell proliferation was determined by quantifying cell number up to 12 days in culture to determine the cell cycle phase of the quiescent population. DiD-labeled PC3-NW1 cells were seeded at 6000/cm^2 into a Permanox Lab-Tek Chamber Slide System (Thermo Fisher Scientific, Waltham, MA, USA) and subcultured for 14 days. Mouse anti-human Ki-67 antibody (BD Biosciences) was then used to identify the growing cells according to the manufacturer's protocol. The fraction of Ki-67+ to Ki-67− cells was analyzed using the FACSCalibur flow cytometer and compared between the DiD+ and DiD− populations.

TaqMan custom array

Mitotically quiescent and rapidly dividing cells were isolated on day 14 by fluorescence-activated cell sorting (FACS), and total RNA was extracted using the ReliaPrepRNA Cell Miniprep System (Promega). cDNA was synthesized using SuperScript III Reverse Transcriptase (Invitrogen, Life Technologies, Carlsbad, CA, USA) with a 1:1 mix of Oligo(dT) 15 and Random Primers (Promega), and samples were analyzed using a 96-gene TaqMan Low Density Array (Applied Biosystems, Foster City, CA, USA) with an Applied Biosystems 7900HT Real-Time PCR System (50°C for 2 minutes, 94.5°C for 10 minutes, 97.0°C for 30 seconds, and 59.7°C for 1 minute, repeated 40 times), covering markers of stem cells, HSC niche components, epithelial-to-mesenchymal transition (EMT), extracellular matrix (ECM), and osteomimicry (complete list is in Supplemental Tables 1 and 2). Data were analyzed using the cycle threshold (CT) relative quantification method with the Applied Biosystems SDS 2.3 software. Quantification of the target cDNAs in all samples was normalized to the endogenous control gene, *GAPDH* (glyceraldehyde 3-phosphate dehydrogenase): $\Delta CT = CT_{target} - CT_{GAPDH}$. The difference in expression for each target cDNA between the quiescent/nonquiescent cells was expressed as ΔΔCT: $\Delta\Delta CT = \Delta CT_{quiescent} - \Delta CT_{nonquiescent}$. The relative expression levels (fold changes) were then calculated using 2 to the power of the ΔΔCT ($2^{-\Delta\Delta CT}$); a 2-fold expression change between cell types was deemed significant (Supplemental Table 2).

Immunofluorescence staining

DiD-labeled prostate cancer cells were subcultured for 14 days and cytospun onto slides. The cells were formalin fixed and stained with anti-human C-X-C chemokine receptor type 4 (CXCR4) phycoerythrin-conjugated mAb (Clone 12G5) or mouse IgG2A isotype control (R&D Systems, Minneapolis, MN, USA) for 1 hour at 20°C. For intracellular staining of matrix metalloproteinase (MMP)-3 (using mouse monoclonal anti-MMP3 antibody) and follistatin (using mouse monoclonal anti-follistatin antibody) (Abcam, Cambridge, United Kingdom), the formalin-fixed cells were permeabilized first in 0.5% Tween diluted in PBS and incubated with primary antibodies or isotype controls overnight at 4°C, followed by 30-minute incubation with Goat anti-mouse IgG secondary antibody (Alexa Fluor 488; Abcam). All samples were then counterstained with DAPI and imaged with a Leica AF6000 time-lapse microscope (Leica Microsystems). The intensity of the immunofluorescence was then quantified with ImageJ software (National Instiutes of Heath, Bethesda, MD, USA) and compared between DiD+ and DiD− populations.

Mitotically quiescent cells *in vivo*

Mice

Male BALB/c nude immunocompromised mice (Charles River Laboratories, Wilmington, MA, USA) were used, and all procedures complied with the United Kingdom Animals (Scientific Procedures) Act 1986 (PPL 40/3462).

Intracardiac injection of tumor cells

PC3-NW1 cells were stained with 5 μM DiD, and single-cell suspensions of 1×10^5 DiD-labeled PC3 cells/100 μl PBS were injected into the left cardiac ventricle [intracardiac/intracardially (i.c.) injection] of 6-week-old male BALB/c nude mice. Tumor growth was monitored for 6 weeks postinjection using *in vivo* imaging systems (IVIS; PerkinElmer, Waltham, MA, USA) for detection of PC3-NW1 and the Illumatool Lighting System (LightTools Research, Encinitas, CA, USA) for detection of PC3-GFP. Cohorts of animals ($n > 6$ per group) were euthanized at different times postinjection. DiD-labeled LNCaP and C4 2B4 cells were also injected (i.c.) into 6-week-old male BALB/c nude mice, and animals were killed at 7 days postinjection to confirm the presence of quiescent tumor cells in bone microenvironment.

Multiphoton (2-photon) microscopy

Dissected tibias were snap frozen in liquid nitrogen, embedded in Cryo-M-Bed compound, and trimmed longitudinally to expose bone marrow area using a cryostat (Bright Instrument Company Limited, Huntingdon, United Kingdom). A stack area of 2104 × 2525 μm below the growth plate with 100 μm in

depth was imaged (Zeiss LSM510 NLO 1-photon microscope; Carl Zeiss Microscopy Ltd., Cambridge, United Kingdom) and reconstructed with the LSM software 4.2 (Carl Zeiss Microscopy Ltd.) as previously described (12). A 633 and 543 nm HeNe laser was used to detect DiD and CM-DiI cells, respectively. The bone and PC3-GFP cells were detected using the 900 nm Chameleon multiphoton laser (Coherent, Santa Clara, CA, USA). The quantitative data and tumor cell number, size, and distance from cell centroid to bone surface were then analyzed by Volocity 3D Image Analysis Software 6.01 (PerkinElmer).

Disruption of the CXCR4 signaling *in vivo*

DiD-labeled 1×10^5 PC3-NW1 cells were i.c. injected into 6-week-old male BALB/c nude mice. At 7 days postinjection, animals were subjected to 5 days of treatment with CXCR4 inhibitor AMD3100 (5 mg/kg, daily intraperitoneal. injection; Sigma-Aldrich) or with PBS control. Animals were then killed, and the presence of DiD-labeled tumor cells was examined and quantified using 2-photon microscopy in tibias *ex vivo*.

Comparison of the tumor-forming ability of the quiescent and nonquiescent subpopulations

PC3-NW1 cells were stained with 5 μM DiD, subcultured, and maintained at a density of at least 5×10^5 cells/cm^2 for 14 days. The DiD+ quiescent and DiD− fast-growing subpopulations were sorted by the FACSAria Cell Sorter (BD Biosciences). DiD+ quiescent cells were injected (i.c.) into 6-week-old male BALB/c nude mice (5×10^3 cells per mouse; $n = 15$). DiD− nonquiescent cells were restained with another lipophilic dye, CellTracker CM-DiI (Life Technologies), before injection (i.c.) into age-matched mice at 2 different concentrations [5×10^3 cells per mouse ($n = 15$) and 1×10^5 cells per mouse ($n = 10$)], to allow tracking by 2-photon microscopy. A control, unsorted population of PC3-NW1 cells was passed through the FACSAria, and 1×10^5 of these cells were labeled with DiD and injected (i.c.; $n = 10$). Tumor growth was monitored up to 6 weeks postinjection by bioluminescent imaging (IVIS), and the tumor burden was evaluated using the Living Imaging *In Vivo* Imaging software (PerkinElmer) based on photon radiance. The presence of tumors was confirmed postmortem by standard histology (Supplemental Fig. 1). The presence of DiD+/CM-Dil+ cells was also determined in tibias using 2-photon microscopy postmortem.

Statistical analysis

All data are expressed as means ± SEM. Statistical significance was tested using an unpaired Student's t test with or without Welsh's correction or 1-way ANOVA with *post hoc* Tukey test as appropriate using the Prism 6 software (GraphPad Software, La Jolla, CA, USA). $P < 0.05$ was considered to be significant.

RESULTS

Prostate cancer cell lines contain mitotically quiescent cell populations at low frequencies

PC3-NW1, LNCaP, and C4 2B4 cells were stained with DiD and followed for up to 3 weeks by flow cytometry. The proportion of cells labeled with DiD (percent DiD+) did not change during the first 3 days but rapidly declined to a steady level of dye retention by day 14. At this and later time points, a dye-retentive population was present at a low frequency (<2%) (**Fig. 1*A–C***). To test whether loss of dye was a result of proliferation (Fig. 1*A*), cell division was inhibited in some cultures by treatment with Mitomycin C. This resulted in dye retention in a high percentage of cells. Cell proliferation under standard conditions was unaffected by DiD treatment (Fig. 1*D*).

To test the viability and proliferative potential of quiescent cells, cells that had retained DiD for 14 days in standard cultures were isolated by FACS and recultured at clonal density. The cells attached to dishes within 24 hours and remained as single cells for 3–5 days. After this time, cells started to form colonies in which dye was sequentially lost in most but not all cells (Fig. 1*E*). This suggests that DiD-retaining populations isolated by FACS remained viable and after a short delay, regained the ability to divide when cultured at low density. The retention of dye by some cells and its loss in most (Fig. 1*E*, day 10) may suggest some asymmetry in proliferation with some cells remaining relatively quiescent.

When DiD-retaining cells and proliferating cells were separated by FACS, dye-retaining cells showed heterogeneity in proliferative marker Ki-67 with both negative and positive staining within the population. However, the percentage of cells that were Ki-67+ was significantly lower in the DiD-retaining population than in the proliferating cells (Fig. 1*F, G*).

Mitotically quiescent populations have a distinctive gene expression profile

The TaqMan custom arrays defined clear and significant differences in the genes expressed by quiescent (dye retaining) and nonquiescent populations isolated by FACS. In particular, type 1 collagen, CXCR4, fibronectin, follistatin, matrilin 2, MMP 2 and 3, prostate stem cell antigen (PSCA), TMPRSS2, tenascin 3, and vitronectin were expressed at >2.5-fold higher levels in the quiescent population compared to the nonquiescent cells. Of the other potential HSC niche components (13), the expression of Tie2 and JAG1 was raised but not significantly in the quiescent cells (**Fig. 2*A*** and Supplemental Table 1). The expression of melanoma cell adhesion molecule (MCAM; CD146) and nestin was significantly lower in quiescent compared to the nonquiescent cells. Although the quiescent cells expressed putative prostate stem cell markers, CD44, and integrins $\alpha 2/\beta 1$, there were no significant differences between expression levels in these cells compared to the proliferating population (Fig. 2*B*). Expression of a further prostate stem cell marker, CD133, was very low in both populations (CT <35 cycles).

The presence of protein encoded by 3 genes that were differentially expressed between DiD-retaining and proliferating cells in the low-density arrays, CXCR4, follistatin, and MMP3 was assessed by immunofluorescent staining of cytospin preparations from mixed cultures (Fig. 2*C*). Comparisons from multiple experiments showed that DiD+ cells expressed high levels of CXCR4 staining. However, there were no correlations between the presence of the other antigens and the transcript levels of the genes encoding these proteins or any associations with the quiescent phenotype (Fig. 2*C–F*).

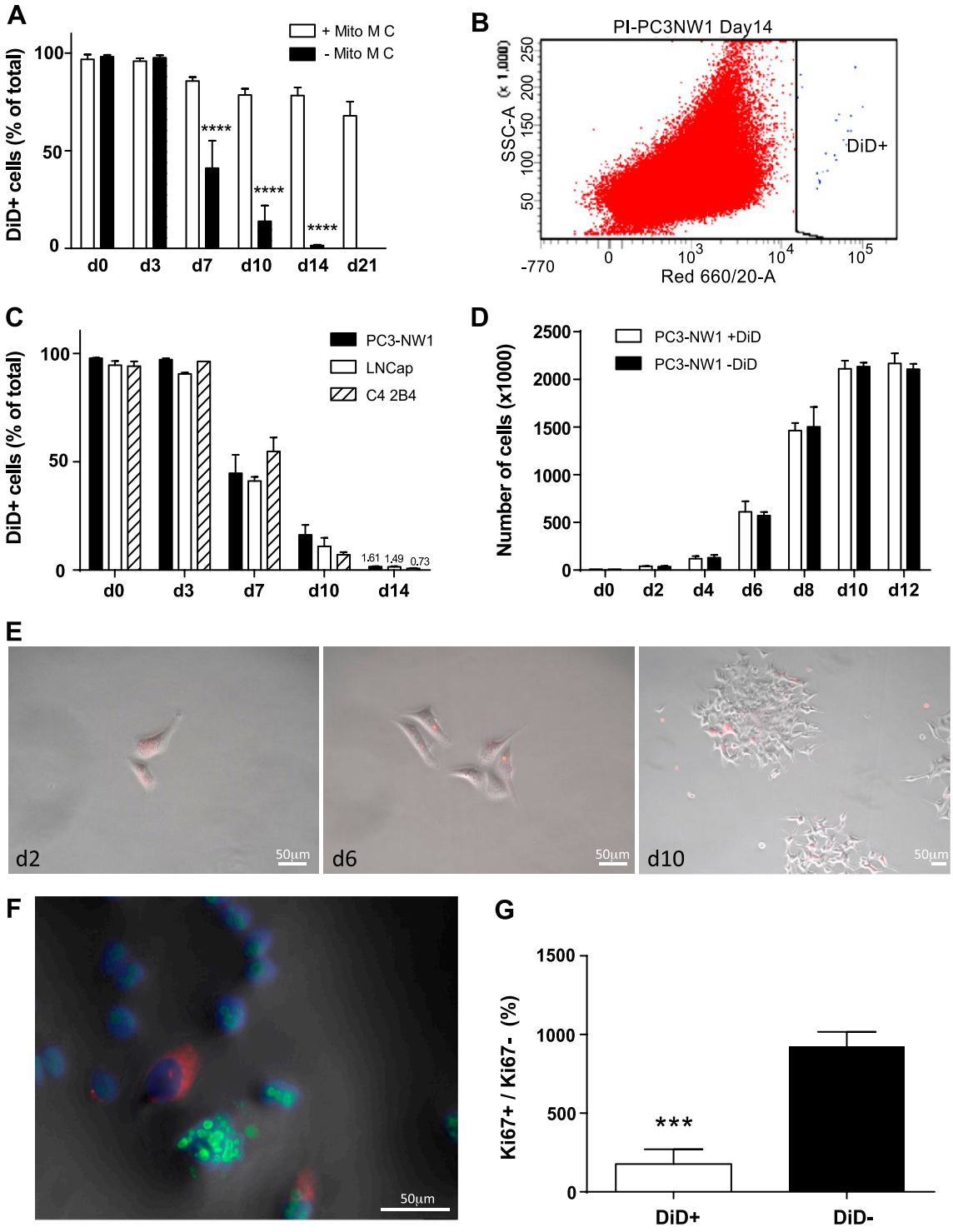

Figure 1. Defining the mitotically quiescent population in prostate cancer cell lines. *A*) Analysis of the retention of DiD labeling in cultures of PC3-NW1 cells in the presence and absence of Mitomycin C (Mito M C) for up to 3 weeks by flow cytometry ($n = 3$). ****$P < 0.0001$, Student's t test. *B*) A representative dot plot of flow cytometry gating shows a distinct population of prostate cancer cells that maintain DiD labeling after 14 days of culture. *C*) Dye content (percent DiD+) of PC3-NW1, LNCaP, and C4 2B4 stained with DiD was followed and analyzed for 14 days by flow cytometry ($n = 3$). *D*) The effects of DiD labeling on proliferation over standard growth curves up to 12 days in culture ($n = 3$). *E*) Cells that retained DiD for 14 days were isolated by FACS and recultured at clonal density. Immunofluorescence microscopy was used to visualize DiD+ cells at day 2, 6, and 10 postseeding. *F*) Immunofluorescent image of a mixed population with dye-retaining cells (DiD+, red) and proliferating cells (DiD−) was immunostained with mouse anti-human Ki-67 antibody (green) and counterstained with DAPI (blue). *G*) Comparison of the percentage of Ki-67 positivity between DiD+ and DiD− populations by flow cytometry analysis ($n = 3$). ***$P < 0.001$, Student's t test.

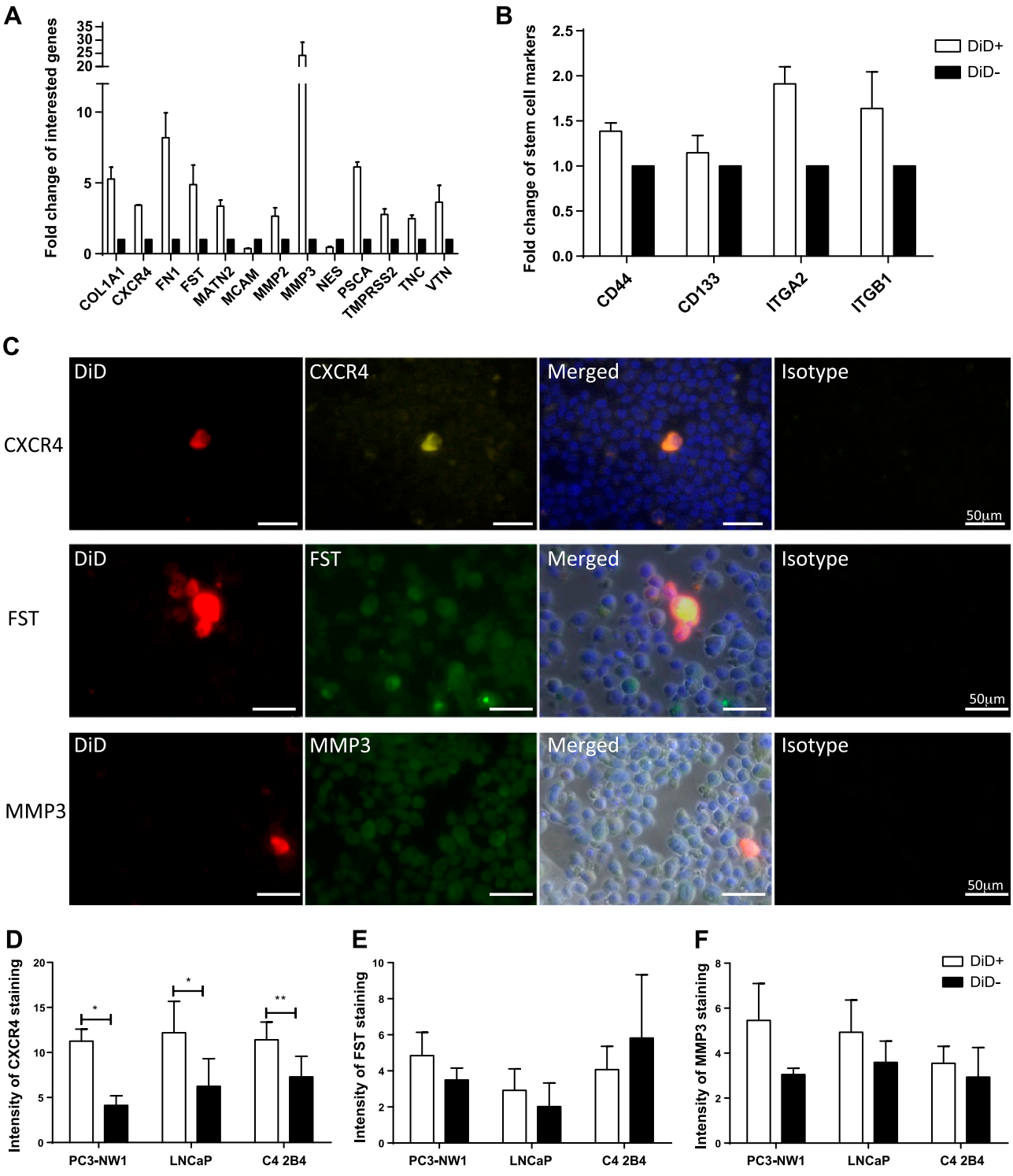

Figure 2. Characterization of quiescent *vs.* nonquiescent cells. *A*) Fold differences in expression of connective tissue proteins, markers of EMT, and HSC niche molecules compared between quiescent *vs.* nonquiescent cells. ΔCT was relative to the housekeeping gene (*GAPDH*) measured by qRT-PCR in low-density arrays ($n = 3$; significant changes were fold differences >2 or <0.5). COL1A1, type 1 collagen; FN1, fibronectin 1; FST, follistatin; MATN2, matrilin 2; NES, nestin; TNC, tenascin 3; VTN, vitronectin. *B*) Fold differences in expression of putative cancer stem cell markers compared between quiescent *vs.* nonquiescent cells. ΔCT was relative to the housekeeping gene (*GAPDH*) measured by qRT-PCR in low-density arrays ($n = 3$; significant changes were fold differences >2 or <0.5) ITGA2, integrin α2; ITGB1, integrin β1. *C*) Immunofluorescence staining shows that DiD-labeled, quiescent PC3-NW1 cells (red) correlated with higher expression of CXCR4 protein (PE+, green) but neither FST (green) nor MMP3 (green) following 14 days of culture after the initial DiD staining. The immunofluorescence staining intensity of (*D*) CXCR4, (*E*) FST, and (*F*) MMP3 was quantified with ImageJ software and compared between DiD+ and DiD− populations ($n = 3$). *$P < 0.05$ and **$P < 0.01$, paired Student's *t* test.

Inhibition of CXCR4 alters the association of tumor cells with bone surfaces

We were able to determine the distribution of tumor cells *in vivo* by prestaining populations with DiD and examining tibias *ex vivo*, by 2-photon microscopy. Animals injected with all 3 prostate cancer cell lines showed DiD-labeled cells present in bone, signals that were absent from naive mice (**Fig. 3*A***). Cells arrived in the tibia within 24 hours, accumulated during the first week, and then declined slowly over the following weeks (Fig. 3*B*). However, DiD+ quiescent cells were still detectable in bone at 6 weeks. Tumor growth was monitored by bioluminescence because PC3-NW1 cells expressed luciferase. Growing lesions were generally detected after 3–4 weeks postinjection. The positions of tumor cells relative to bone were mapped and were shown to be in close proximity to bone (within 40 μm); however, there was a gradual but not significant increase in the distance from bone structures with time (Fig. 3*C*).

To test the functional involvement of CXCR4 signaling in the retention of tumor cells within bone, cohorts of animals were treated with an agent that interferes with CXCR4 signaling (AMD3100) 1 week after injection with tumor cells (schematic in Fig. 3*D*). This resulted in a significant shift in the positioning of tumor cells relative to bone surfaces (Fig. 3*E*). There was no significant reduction in the total number of tumor cells detected within bone (Fig. 3*F*), suggesting that tumor cells were not mobilized back into the circulation by this treatment.

The mitotically quiescent phenotype *in vitro* is more tumorigenic *in vivo* than proliferating cells

We tested the hypothesis that the quiescent population, present *in vitro*, was more tumorigenic *in vivo*. To do this, 5×10^3 mitotically quiescent cells (DiD+) or proliferating cells (DiD− on sorting, restained with CM-Dil so they could be tracked *in vivo*) were injected (i.c.) into 6-week-old animals to evaluate their tumorigenicity (**Fig. 4*A***). Animals were culled between 6 and 10 weeks postinjection of tumor cells, depending on the severity of tumor burden. At this stage, both DiD+ and CM-Dil+ cells (sorted as DiD−) were present as single cells within the tibias examined by 2-photon microscopy using channels that discriminated DiD/CM-DiI-labeled cells (Fig. 4*B*). There were no DiD-labeled cells detected among those labeled with CM-Dil. Neither the FACS nor CM-DiI staining affected the tumorigenicity of PC3-NW1 because injection of 10^5 unsorted cells or sorted CM-DiI-restained cells produced high frequencies of growing tumors in skeleton (>80%) as in previous studies. This confirms that dye staining and FACS treatment did not affect tumor formation rates.

Injection of 5×10^3 DiD− cells formed skeletal lesions in only 15% of animals, with no long bone lesions. Injection of 5×10^3 DiD+ cells produced tumors in 55–60% of animals, and tumors were observed in long bone at week 6 postinjection *via* the IVIS system and further anatomic confirmation postmortem (Fig. 4*C*). Analyzed using the Living Imaging *In Vivo* Imaging software, both the number of tumors in bone per mouse and the total bone tumor burden (photon radiance) of each mouse were both statistically significantly higher in the group of mice injected with DiD+ cells (Fig. 4*D*, *E*), further confirming the higher tumorigenicity of quiescent cells in skeleton. In animals injected with 5000 cells, the DiD+ cell numbers were too low to accurately quantify either by 2-photon microscopy within tibias or by flushing bones and analyzing suspensions by FACS. Interestingly, there were no tumors present in nonskeletal sites in animals injected with cells that retained DiD for 14 days in cell culture, whereas soft tissue tumors were seen in those that were injected with DiD− sorted populations.

DISCUSSION

Two key findings have been demonstrated in these studies. First, we have shown that the widely used human prostate cancer cell lines PC3 and LNCaP and its variant C4 2B4 contain populations of cells that are slow growing/quiescent but not specifically stem like. These cells are present in cultures where the majority of the population grows rapidly under standard conditions. Second, when this population was isolated from PC3-NW1 cells, it was able to form skeletal tumors more frequently than the more rapidly dividing population, when injected into immunosuppressed animals. We (12) and others have recently used this technology to identify slow-growing cell populations in the PC3 cell line (14), but the latter have not characterized separate cell populations as we have done here.

We compared gene expression profiles of quiescent and proliferating populations using a low-density array technology. The quiescent population *in vitro* expressed higher levels of CXCR4 and contained higher levels of this protein, measured by immunofluorescence, than nonquiescent cells. CXCR4 has been implicated in PC3 cell migration (10) and is required for the quiescence of HSC (15). The present study has identified CXCR4 as a marker of quiescent cells in a population with an increased ability to form tumors in animals. Disruption of CXCR4 signaling using its antagonist AMD3100 did suggest that cells were induced to move away from bone surfaces and potentially away from osteoblast lineage cells, a known source of the ligand SDF1 (CXCL12). This implies involvement of this signaling system in the homing process, as suggested by others using these models (10), where this treatment was shown to result in tumor cells reentering the circulation. We did not see any reduction of tumor cell numbers in bone in our study that would have been indicative of remobilization of tumor cells to the circulation, nor did we see an increase in circulating tumor cells in treated animals. That there was no significant reduction in DiD+ cell numbers in AMD3100-treated animals would also indicate that tumor colony formation did not increase with this treatment.

Although the expression of other genes in the selected arrays was increased, this did not appear to be reflected in increases in specific protein levels, apart from CXCR4. There may be a number of reasons for this. First, there may be genuinely no increased protein production associated with the elevated transcript levels observed. Alternatively, we may not have chosen the correct time window to observe increased protein levels, or the assays were not sensitive enough to detect differences. However, the relationship between elevated expression of some of the other genes

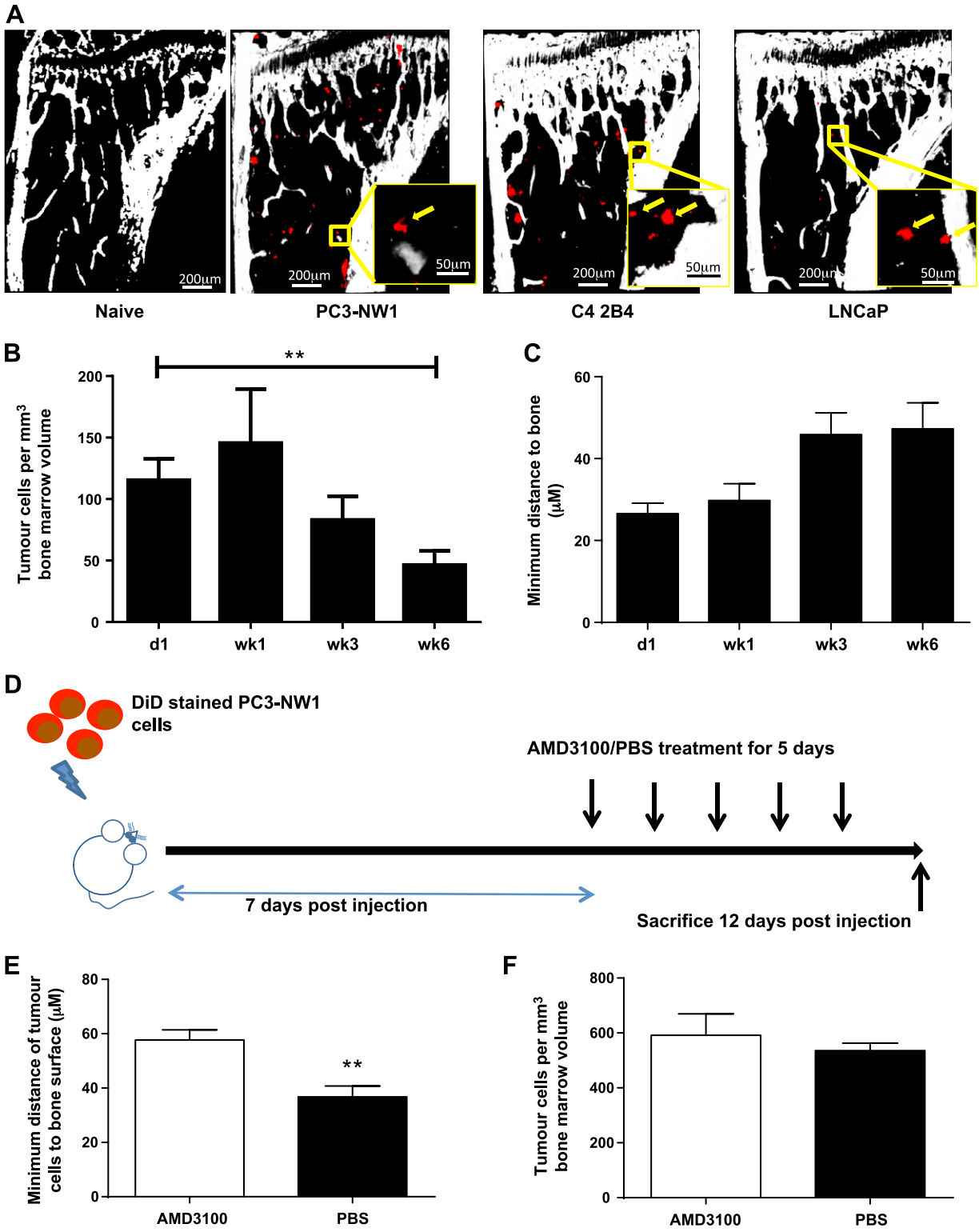

Figure 3. Disruption of CXCR4 interactions induces a shift in tumor cell position in bone. *A*) Two-photon scans of tibias from naive mice and mice injected (i.c.) with DiD-labeled PC3-NW1, C4 2B4, and LNCaP cells 7 days postinjection. DiD-labeled cells are indicated by yellow arrows. *B*) Frequency of DiD-labeled tumor cells per cubic millimeter bone marrow detected by 2-photon microscopy in tibias of a cohort of mice injected (i.c.) with PC3-NW1 cells over 6 weeks postinjection ($n > 6$). $^{**}P < 0.01$, 1-way ANOVA with *post hoc* Tukey test. *C*) The position of tumor cells relative to bone surfaces over time mapped using the Volocity 3D Image Analysis Software ($n > 6$). *D*) Schematic outline of the procedure used to inhibit CXCR4 and evaluate the association of tumor cells and bone: 6-week-old athymic mice were injected (i.c.) with DiD-labeled PC3-NW1, and daily treatments of CXCR4 antagonist (AMD3100) were started 7 days postinjection for 5 consecutive days. The mice were then killed 24 hours later for 2-photon microscopy analysis. *E*) The distance from tumor cells to the nearest bone surface and (*F*) the number of DiD-labeled tumor cells per cubic millimeter bone marrow were compared between the AMD3100-treated and control animals ($n = 8$). $^{**}P < 0.01$, Student's *t* test; ns, not significant.

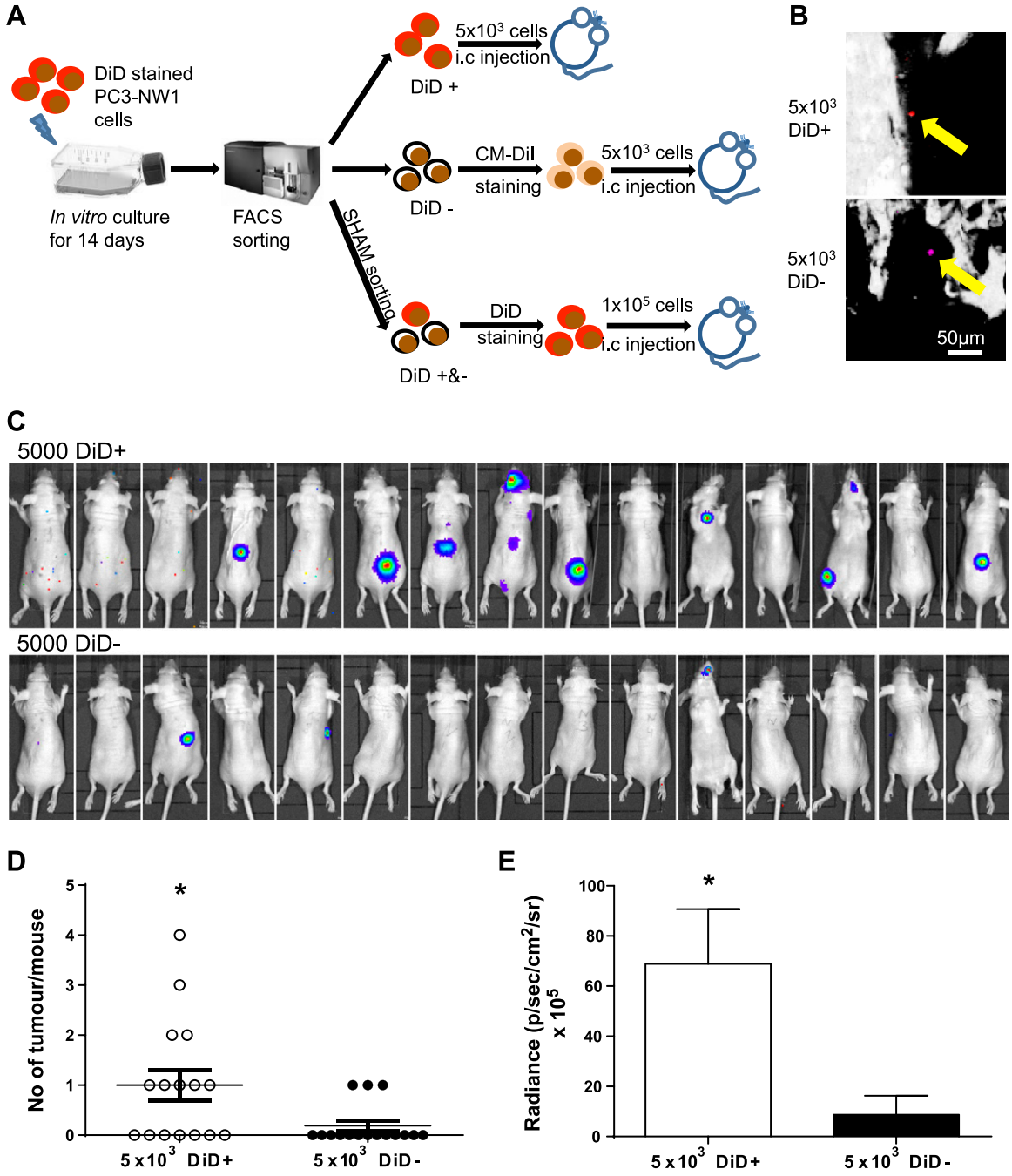

Figure 4. Assessment of the growth and tumor-initiating capacity of mitotically quiescent prostate cancer cells *in vivo*. *A*) Schematic outline of the procedure used to isolate and evaluate the tumorigenicity of mitotically quiescent and dividing cells *in vivo*: PC3-NW1 cells, which constitutively expressed luciferase, were stained with DiD and cultured continuously in standard medium for 14 days. DiD-retaining (DiD+) and -nonretaining (DiD−) cells were fluorescence-activated cell sorted, and DiD− cells were restained with CM-Dil. Different populations were then injected i.c. into athymic mice including mitotically quiescent (DiD+; 5×10^3 cells per mouse), nonquiescent populations (DiD−; 5×10^3 cells per mouse), and the whole, mock-sorted population (1×10^5 cells per mouse). CM-Dil was used for the restaining of DiD− cells to exclude the possibility of missorted DiD+ populations being retained in small numbers in the former population and identified in tibias following injection. *B*) DiD+ (upper panel) or CM-DiI (DiD−; lower panel)-labeled tumor cells were visualized in tibias by 2-photon microscopy (arrows) 6 weeks postinjection. *C*) The tumorigenicity in the skeleton, especially in long bone, was visualized by bioluminescence for 6 weeks postinjection using the IVIS system and compared between groups injected with DiD+ and DiD− cells (both $n = 15$). *D*) The number of tumors per mouse and (*E*) tumor burden (photon radiance) were analyzed and compared between the 2 groups using the Living Imaging In Vivo Imaging software ($n = 15$). *$P < 0.05$, Student's t test.

and cell migration/metastasis may be still worth considering. Of the other genes that were significantly up-regulated as measured by quantitative RT-PCR (qRT-PCR) in the quiescent cell population, MMP3 is linked to the expression of CXCR4. This protease has been shown to be elevated in the serum of patients with metastatic prostate cancer (16),

and its inhibition by treatment of animals with TIMP3 suppressed the formation of PC3 tumors (17). Others have shown that MMP3 expression is induced by CXCR4 signaling (18). MMP2 has been shown to be present in patient bone biopsies and in PC3 xenografts where it has been revealed to induce recruitment of osteoclasts/participate in the formation of lytic bone disease (19). Others have shown that experimentally induced expression of αVβ6 integrin increased MMP2 production by PC3 cells and promoted osteolytic activity *in vivo* (20). The expression of fibronectin, a binding partner for αVβ6 integrin, was also increased in the quiescent cells. Fibronectin is induced in EMT and has been associated with metastatic phenotype in breast cancer (21) as well as in prostate cancer cells (22) where overexpression of miR200b inhibited EMT, metastasis, and down-regulated fibronectin expression. Vitronectin has been associated with metastasis in breast cancer where binding of αVβ3 integrin facilitated invasion under hypoxic conditions (23). Associations of vitronectin with this integrin have also been implicated as a driver of adhesion and invasion in prostate cancer (24). The present study would suggest that autologous production of ECM glycoproteins is a part of the quiescent, metastasis-initiating phenotype. Similarly, tenascin C, which is produced by PC3 cells and expression elevated in the quiescent cells in our study, has been variably linked to reactive stroma in prostate cancer progression (25). The TMPRSS2 gene expression was elevated in the mitotically quiescent population, but there was no expression of transcripts indicating fusion of this gene with the erythroblast transformation-specific (ETS) family member ETS-related gene. Although much attention in prostate research has focused on the fusion discussed above, the protein encoded by TMPRSS2 is a transmembrane serine protease, and it is possible that this could have a role in tumor cell migration/formation of metastases in a cell type we have shown to have an increased capacity to form tumors in bone.

The present study suggested that the quiescent population in the PC3-NW1 cell line did not specifically share the full putative prostate stem cell phenotype (1). In particular, the quiescent cells did not express CD133 but did express high levels of integrin β1 and CD44 (CT values <25). However, there were no significant differences in the levels of expression of these markers between quiescent and nonquiescent cells.

The findings with respect to CD44 and integrin β1 are very much in line with those reported elsewhere with the PC3 cell line: CD44 protein is present on $>60\%$ of PC3 cells (26), and α2/β1 integrin staining is also ubiquitous in this cell and not confined to a small subpopulation. In PC3 cells, the regulatory regions associated with the CD133 gene have been shown to be hypermethylated and the transcript levels shown to be low/undetectable in the whole population (27). Although we did not have a positive control for CD133 expression in our arrays, we did look for CD133 with 2 independent primer sets and failed to find expression of this gene in either DiD+ or DiD− cells.

In contrast, the expression of PSCA was elevated in the quiescent population. This protein is highly expressed in prostate cancer compared to normal tissues and has been associated with tumor progression (28, 29). We conclude that whereas the quiescent population carries some stem cell markers, these do not uniquely identify this population. It is quiescence itself that is specifically associated with an increased capacity to form metastatic lesions in xenograft models.

Taken together, the gene expression profiling data presented in this study suggest that the cells that are quiescent *in vitro* express higher levels of transcripts consistent with an invasive, metastatic phenotype. How and why this rare population is present or is generated *in vitro* remain to be discovered.

The *in vivo* studies clearly demonstrated that the quiescent cells isolated from cell cultures were more tumorigenic in initiating tumors in bone than rapidly dividing populations. This suggests that the quiescent population contains higher numbers of cells capable of surviving in the circulation, homing to the bone marrow, and eventually being activated to form growing lesions.

Our studies suggest that mitotic quiescence, as defined by retention of the DiD dye for long periods, is in itself a marker for an increased ability to form metastases in experimental animals. These cells carry some of the putative prostate cancer stem cell markers suggested by others, but these are not exclusive to the quiescent phenotype. The consistently increased expression of CXCR4 in the quiescent population would enhance migration to bone for this cell type, which may, in part, provide an explanation for the increased capacity of these cells to generate lesions in bone. The presence of increased levels of this protein in tumor populations may be useful in predicting their capacity for migration and metastasis formation. In our previous studies, we have highlighted problems in detecting CXCR4 in prostate cancer tissues (7). In particular, we showed that the staining patterns reported were prone to artifact and that the overall frequency of CXCR4 staining was low in prostate tissues. To date, there have been no definitive, properly validated studies using primary prostate cancer tissue arrays with good clinical follow-up to test the hypothesis that the presence of CXCR4 in subpopulations of cells in these tissues predicts the presence of occult metastases in patients. Our studies and others (10) would suggest that this now needs to be given priority, especially where patients are being diagnosed with early-stage disease and for whom prognosis is currently not clearly defined.

In conclusion, our study is the first to show that mitotic quiescence identifies cells with the highest capacity to form bone metastases in prostate cancer models. This is counterintuitive in that it might be expected that rapidly growing populations would be more capable of forming lesions. However, our studies show that the quiescent phenotype, with its consistent gene expression profile, in particular the production of CXCR4, allows cells to survive and home to bone where mitotic quiescence persists until proliferation is initiated. FJ

The authors thank Cancer Research UK for its generous financial support and Yorkshire Cancer Research for funding *in vivo* imaging equipment (IVIS). The authors are grateful to the following for technical support: Miss Orla Gallagher, Mr. Darren Lath, Susan Clark, and Kay Hopkins. P.I.C. is supported by Mrs. Janice Gibson and the Ernest Heine Family Foundation. The authors declare no conflicts of interest.

REFERENCES

1. Collins, A. T., Berry, P. A., Hyde, C., Stower, M. J., and Maitland, N. J. (2005) Prospective identification of tumorigenic prostate cancer stem cells. Cancer Res. **65**, 10946–10951
2. Pellacani, D., Oldridge, E. E., Collins, A. T., and Maitland, N. J. (2013) Prominin-1 (CD133) expression in the prostate and prostate cancer: a marker for quiescent stem cells. *Adv. Exp. Med. Biol.* **777**, 167–184
3. Sheng, X., Li, Z., Wang, D. L., Li, W. B., Luo, Z., Chen, K. H., Cao, J. J., Yu, C., and Liu, W. J. (2013) Isolation and enrichment of PC-3 prostate cancer stem-like cells using MACS and serum-free medium. Oncol. Lett. **5**, 787–792
4. Williamson, S. C., Hepburn, A. C., Wilson, L., Coffey, K., Ryan-Munden, C. A., Pal, D., Leung, H. Y., Robson, C. N., and Heer, R. (2012) Human α(2)β(1)(HI) CD133(+VE) epithelial prostate stem cells express low levels of active androgen receptor. *PLoS One* **7**, e48944
5. Guzmán-Ramírez, N., Voller, M., Wetterwald, A., Germann, M., Cross, N. A., Rentsch, C. A., Schalken, J., Thalmann, G. N., and Cecchini, M. G. (2009) *In vitro* propagation and characterization of neoplastic stem/progenitor-like cells from human prostate cancer tissue. *Prostate* **69**, 1683–1693
6. Colombel, M., Eaton, C. L., Hamdy, F., Ricci, E., van der Pluijm, G., Cecchini, M., Mege-Lechevallier, F., Clezardin, P., and Thalmann, G. (2012) Increased expression of putative cancer stem cell markers in primary prostate cancer is associated with progression of bone metastases. *Prostate* **72**, 713–720
7. Eaton, C. L., Colombel, M., van der Pluijm, G., Cecchini, M., Wetterwald, A., Lippitt, J., Rehman, I., Hamdy, F., and Thalman, G. (2010) Evaluation of the frequency of putative prostate cancer stem cells in primary and metastatic prostate cancer. *Prostate* **70**, 875–882
8. Germann, M., Wetterwald, A., Guzmán-Ramirez, N., van der Pluijm, G., Culig, Z., Cecchini, M. G., Williams, E. D., and Thalmann, G. N. (2012) Stem-like cells with luminal progenitor phenotype survive castration in human prostate cancer. *Stem Cells* **30**, 1076–1086
9. Polson, E. S., Lewis, J. L., Celik, H., Mann, V. M., Stower, M. J., Simms, M. S., Rodrigues, G., Collins, A. T., and Maitland, N. J. (2013) Monoallelic expression of TMPRSS2/ERG in prostate cancer stem cells. *Nat. Commun.* **4**, 1623
10. Shiozawa, Y., Pienta, K. J., and Taichman, R. S. (2011) Hematopoietic stem cell niche is a potential therapeutic target for bone metastatic tumors. *Clin. Cancer Res.* **17**, 5553–5558
11. Pece, S., Tosoni, D., Confalonieri, S., Mazzarol, G., Vecchi, M., Ronzoni, S., Bernard, L., Viale, G., Pelicci, P. G., and Di Fiore, P. P. (2010) Biological and molecular heterogeneity of breast cancers correlates with their cancer stem cell content. *Cell* **140**, 62–73
12. Wang, N., Docherty, F. E., Brown, H. K., Reeves, K. J., Fowles, A. C., Ottewell, P. D., Dear, T. N., Holen, I., Croucher, P. I., and Eaton, C. L. (2014) Prostate cancer cells preferentially home to osteoblast-rich areas in the early stages of bone metastasis—evidence from *in vivo* models. *J. Bone Miner. Res.* **29**, 2688–2696
13. Arai, F., Hirao, A., Ohmura, M., Sato, H., Matsuoka, S., Takubo, K., Ito, K., Koh, G. Y., and Suda, T. (2004) Tie2/angiopoietin-1 signaling regulates hematopoietic stem cell quiescence in the bone marrow niche. *Cell* **118**, 149–161
14. Yumoto, K., Berry, J. E., Taichman, R. S., and Shiozawa, Y. (2014) A novel method for monitoring tumor proliferation *in vivo* using fluorescent dye DiD. *Cytometry A* **85**, 548–555
15. Nie, Y., Han, Y. C., and Zou, Y. R. (2008) CXCR4 is required for the quiescence of primitive hematopoietic cells. *J.* Exp. Med. **205**, 777–783
16. Jung, K., Nowak, L., Lein, M., Priem, F., Schnorr, D., and Loening, S. A. (1997) Matrix metalloproteinases 1 and 3, tissue inhibitor of metalloproteinase-1 and the complex of metalloproteinase-1/tissue inhibitor in plasma of patients with prostate cancer. *Int. J. Cancer* **74**, 220–223
17. Zhang, L., Zhao, L., Zhao, D., Lin, G., Guo, B., Li, Y., Liang, Z., Zhao, X. J., and Fang, X. (2010) Inhibition of tumor growth and induction of apoptosis in prostate cancer cell lines by overexpression of tissue inhibitor of matrix metalloproteinase-3. *Cancer Gene Ther.* **17**, 171–179
18. Singh, S., Singh, U. P., Grizzle, W. E., and Lillard, Jr., J. W. (2004) CXCL12-CXCR4 interactions modulate prostate cancer cell migration, metalloproteinase expression and invasion. *Lab. Invest.* **84**, 1666–1676
19. Nemeth, J. A., Yousif, R., Herzog, M., Che, M., Upadhyay, J., Shekarriz, B., Bhagat, S., Mullins, C., Fridman, R., and Cher, M. L. (2002) Matrix metalloproteinase activity, bone matrix turnover, and tumor cell proliferation in prostate cancer bone metastasis. *J.* Natl. Cancer Inst. **94**, 17–25
20. Dutta, A., Li, J., Lu, H., Akech, J., Pratap, J., Wang, T., Zerlanko, B. J., FitzGerald, T. J., Jiang, Z., Birbe, R., Wixted, J., Violette, S. M., Stein, J. L., Stein, G. S., Lian, J. B., and Languino, L. R. (2014) Integrin αvβ6 promotes an osteolytic program in cancer cells by upregulating MMP2. *Cancer Res.* **74**, 1598–1608
21. Nutter, F., Holen, I., Brown, H. K., Cross, S. S., Evans, C. A., Walker, M., Coleman, R. E., Westbrook, J. A., Selby, P. J., Brown, J. E., and Ottewell, P. D. (2014) Different molecular profiles are associated with breast cancer cell homing compared with colonisation of bone: evidence using a novel bone-seeking cell line. *Endocr. Relat. Cancer* **21**, 327–341
22. Williams, L. V., Veliceasa, D., Vinokour, E., and Volpert, O. V. (2013) miR-200b inhibits prostate cancer EMT, growth and metastasis. *PLoS One* **8**, e83991
23. Pola, C., Formenti, S. C., and Schneider, R. J. (2013) Vitronectin-αvβ3 integrin engagement directs hypoxia-resistant mTOR activity and sustained protein synthesis linked to invasion by breast cancer cells. *Cancer Res.* **73**, 4571–4578
24. Cooper, C. R., Chay, C. H., and Pienta, K. J. (2002) The role of alpha (v)beta(3) in prostate cancer progression. *Neoplasia* **4**, 191–194
25. Reinertsen, T., Halgunset, J., Viset, T., Flatberg, A., Haugsmoen, L. L., and Skogseth, H. (2012) Gene expressional changes in prostate fibroblasts from cancerous tissue. *APMIS* **120**, 558–571
26. Draffin, J. E., McFarlane, S., Hill, A., Johnston, P. G., and Waugh, D. J. (2004) CD44 potentiates the adherence of metastatic prostate and breast cancer cells to bone marrow endothelial cells. *Cancer Res.* **64**, 5702–5711
27. Pellacani, D., Packer, R. J., Frame, F. M., Oldridge, E. E., Berry, P. A., Labarthe, M. C., Stower, M. J., Simms, M. S., Collins, A. T., and Maitland, N. J. (2011) Regulation of the stem cell marker CD133 is independent of promoter hypermethylation in human epithelial differentiation and cancer. *Mol. Cancer* **10**, 94
28. Reiter, R. E., Gu, Z., Watabe, T., Thomas, G., Szigeti, K., Davis, E., Wahl, M., Nisitani, S., Yamashiro, J., Le Beau, M. M., Loda, M., and Witte, O. N. (1998) Prostate stem cell antigen: a cell surface marker overexpressed in prostate cancer. *Proc. Natl. Acad. Sci. USA* **95**, 1735–1740
29. Gu, Z., Thomas, G., Yamashiro, J., Shintaku, I. P., Dorey, F., Raitano, A., Witte, O. N., Said, J. W., Loda, M., and Reiter, R. E. (2000) Prostate stem cell antigen (PSCA) expression increases with high gleason score, advanced stage and bone metastasis in prostate cancer. *Oncogene* **19**, 1288–1296

Received for publication November 14, 2014.
Accepted for publication March 25, 2015.